

Kerbala Journal for Engineering Sciences

https://kjes.uokerbala.edu.iq



ISSN: 2709-6718

Prediction of Optimum Intak Angle at Open Channel Junction Using Gene Expression Programing Technique

Batool Mousa Alaa*,1, Abdul khider Mutasher 1, Fatima Mahdi1

¹ Department of Civil Techniques, Kerbala Technical Institute, Al-Furat Al-Awsat Technical University, Kerbala, Iraq.

*Corresponding author, E-mail: <u>batool.mousa.ikr17@atu.edu.iq</u>

Received: 11 March 2025; Revised: 23 August 2025; Accepted: 01 September 2024; publish:30 September

Abstract

Usually, water intakes are used to divert water from the primary canal or river to the tertiary canals and turbine systems. In cases when the flow is being separated at the branch channel's inlet, the flow structure in this area is more intricate than in other parts of the network. For the most part, intakes are built at right angles, which creates a sizable separation zone at the entrance of the subchannel and decreases flow discharge. In order to minimize the separation zone's dimensions, the intake should be positioned at the best possible angle. A numerical study was run in a rectangular channel with a side channel branching off of it to determine the optimal intake angle. To achieved this study, eleven intakes were installed on one side of the main channel at varying angles of 15, 30, 45, 60, 75, 90, 105, 120, 135, 150 and 165 degrees to find the optimum intake position. Additionally, a unique method for estimating the separation zone's dimensions utilizing an advanced microcomputing modeling approach called Gene Expression Programming (GEP) has been proposed as a result of the study's findings. The outcomes of the numerical simulation were then utilize to make a compare between the GEP model and the nonlinear regression model (NLR). As a comparison, high R values and small RMSE and MAE indicate that the empirical formula derived using the GEP program is superior to the NLR formula (R²=0.903, RMSE=0.109, and MAE=0.092).

Keywords: Branching Angle, GEP Model, NLR Model, Shape Index, Separation Zone.

1. Introduction

Water flow structure at intakes is complex and of interest to engineers due to its many uses in turbine intakes, irrigation canals and other water distribution networks such as sewer networks. When

the flow passes through a straight rectangular channel, the streamlines are almost deliberately streamlined with the direction of movement, but as soon as a water intake is placed on the side of the channel, the flow path changes so that the flow lines deviate towards the intake. As a result of the deflection of the flow path, a separation zone is formed at the entrance of the branch channel [1].

ISSN: 2709-6718

Many complicated issues, including local sedimentation, channel scour, and sidewall erosion, accompany the merging of two flows because of production of various hydraulic condition in channel alignment [2]. Recently, the computational fluid dynamics (CFD) has become increasingly popular in recent years as a tool for simulating fluid flow behavior at channel junctions in engineering. Some of the recent studies used the Flow 3D program as a numerical modeling method to simulate the branching flow at the intakes and find the optimal angle from the intake angles like Heydary [3] and some used the laboratory work to find the optimal angle, such as keshavarzi [1]. Where the author Keshavarzi found that the best angle for branching is the angle of 55°, while Haidari found that the angle of 45° is the best angle as it increases the discharge of water [4].

The separation zone forms under the influence of many factors in the field, including branching angle, upstream Froude number, upstream flow depth, flow intensity (the result of dividing the velocity at upstream by the critical velocity of channel), and discharge ratio. Recently, with the development of artificial intelligence (AI) approaches, mathematical computation has advanced to the point that modeling can be performed rapidly, precisely, and with minimal input from the user [5, 6]. Artificial neural networks (ANN), adaptive neural fuzzy inference system (ANFIS), genetic programming (GP), genetic algorithms (GA), and gene expression programming (GEP) are some of the key AI technologies [7, 8].

The GEP Soft Computing Technologies tool is another essential resource, having recently taken the place of numerous other computer software because to its superior simplicity, Run speed, and ease of coding, calculation, and modeling. As a mentioned in the previous studies, several experts in various branches of engineering have demonstrated that AI techniques are more precise and functional than their predecessors [9, 10]. Data from Flow-3D numerical simulations, split into a training and testing data set, was combined with GEP and NLR models to formulate predictions of optimum intake angle. The dimensionless parameters of discharge ratio, flow intensity, upstream Froude number, and upstream flow depth were revealed to be the most relevant variables on predicting optimum angle. Moreover, these dimensionless parameters were used in GEP and NLR models as both output and input variables. It was used the root-mean-square error (RMSE), the mean absolute error (MAE), and the correlation coefficient (R²) to determine the best method for forecasting the optimal intake angle.

2. Dimensional Analysis

The current research identified the upstream velocity flow (Vu), critical flow velocity (Vc), the flow depth at upstream main channel (yu), acceleration due to gravity (g), the fluid density (ρ), the branching channel flow depth (yb), the channel width (B), the upstream discharge (Qu), the branch

channel discharge (Qb), branching angle (θ), and the flow time (t) as the most influential variables affecting separation process. Eleven angles used in this study: 15, 30, 45, 60, 75, 90, 105, 120, 135, 150 and 165 degrees. All angles were installed at one side with respect to the main channel. The functional linkages of general dimensional analysis might be formulated through research into the influential elements and mechanisms affecting separation zone dimensions, it can be written as:

$$\frac{W_S}{L_S} = f_1(\theta, \rho, g, y_u, y_b, B, Q_u, Q_b, T, V_u, V_c)$$
(1)

ISSN: 2709-6718

 $\frac{W_s}{L_s}$: the shape index;

 θ : the branching angle.

 ρ : water density.

g: the gravity.

 y_u : upstream water depth

 y_b : Branch chanel water depth.

B: the Channels depth.

 Q_u : Upstream discharge of main channel.

 Q_b : Branch channel discharge.

T: the time.

 V_u : Upstream velocity.

 V_c : Critical velocity.

The primary objective of dimensional analysis will be to formulate a problem's parameters in such a way that their interrelationships become transparent and it described by the choice of their dimensions. The resulting metric-free function characterizing the factors' effects on separation zone dimensions or on the shape index (Ws/Ls) (the result of diviving the width (Ws) of separation zone by its length (Ls)) was recovered using Buckingham's -theorem and the selection of, V, and B as the repeated variables, as shown in equation 2.

$$\frac{W_s}{L_s} = f_2\left(\theta, F_u, \frac{y_u}{B}, \frac{Q_b}{Q_u}, \frac{V_u}{V_c}\right) \tag{2}$$

Where,

Ws/Ls represent shape index

 θ represents branching angle

Fu represent upstream Froude number

yu/B is upstream flow depth

Vu/Vc is flow intensity

Qb/Qu represents the discharge ratio (Qr)

New shape index formula based on GEP and NLR models was derived using these metric-free parameters.

ISSN: 2709-6718

3. Data Sets of Numerical Work

Intake flow separation has been examined numerically using the Flow-3D model under a wide range of branching angles and flow conditions. In fact, the critical features in the design of intakes have been stated in terms of the maximum dimensions of the separation zone happening at the entrance of the intake using fow-3D models. It was determined that the Flow-3D model was successful in simulating the flow at intake by comparing the results from the Ramamurthy [11] laboratory model to those derived by the corresponding model of Flow-3D software. The numerical simulation model and the laboratory model developed by Ramamurthy [11] were found to be highly validated against one another, with a root mean square error (RMSE) of about 0.055 and a mean absolute error (MAE) of about 0.025. This supports the concept that the flow-3d is a reliable technique for modelling the emergence of a separation zone. Numerical simulation yielded a total of 150 sets, and this data representing the dimensions of the separation zone occurring at the entrance to the intake for a given value of a given parameter depending on the flow velocity, upstream flow depth, discharge ratio, upstream Froude number, and branching angle. Table 1 summarizes the variation in these variables. After splitting the data into a training set (80%) and a validation set (20%), the necessary shape index equation was modeled in GEP and NLR. In the formula for making predictions, the shape index (Ws/Ls) was treated as the dependent parameter while the other data were treated as independent. The best approach for predicting the optimal formula of shape index was then determined by calculating these three statistical measures: RMSE, MAE, and \mathbb{R}^2 .

Table 1: Variables Limitations of GEP Model and NLR Model

Variables	Data Limitations	
	Min. Limit	Max. Limit
Qr	0.15	0.95
Vu/Vc	0.45	1.2
Yu/B	0.08	0.31
Fu	0.3	1.5
θ	15	165

To determine the magnitude of a variable's effect on the size of the separation region, it is crucial to notice that in each attempt one of the variables is evaluated while the rest variables are held constant.

3.1 Influence of Discharge Ratio (Qr)

The discharge ratio is a crucial factor in determining the size of the separation zone (the results of dividing the incoming discharge of the branch channel (Qb) by the discharge of the upstream main channel(Qu)). Iterations were performed with varying branching angles, flow intensities (Vu/Vc), flow depths (yu/B), and upstream Froude numbers (Fu) to demonstrate the effect of the discharge ratio on the separation zone. The length and distribution of the separation zone were shown to increase at high discharge ratios across all branching angles, compared to low discharge ratios. As an example, the impact of discharge ratios on branching flow at an angle of 90 degrees is depicted in the following pictures. As shown in figures 1 to 3, it can be seen that how the dimensions of the separation region developed with variation of shape index for different values of Qr.

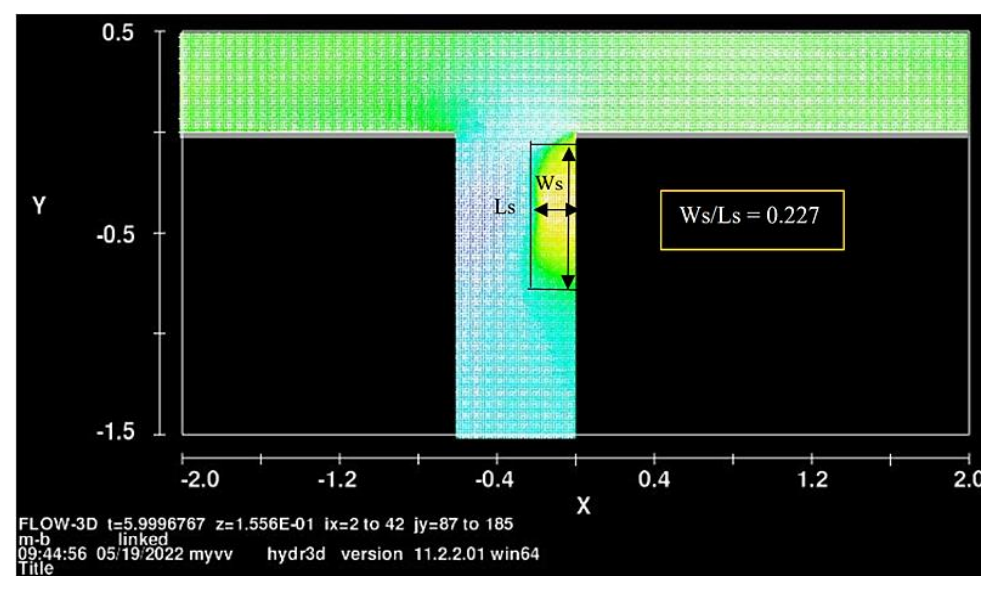


Figure 1: Shape Index at Qr= 0.95, Fu =0.3, Vu/Vc= 0.45, $\theta = 90^{\circ}$, yu/B=0.31

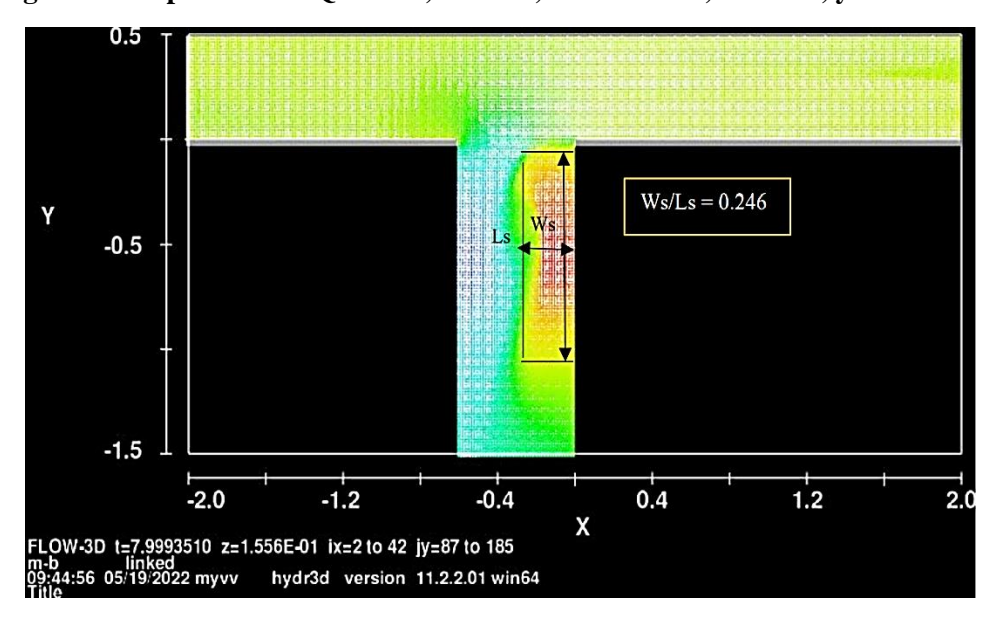


Figure 2: Shape index at Qr=0.55, Fu=0.3, Vu/Vc=0.45, $\theta = 90^{\circ}$, yu/B=0.31

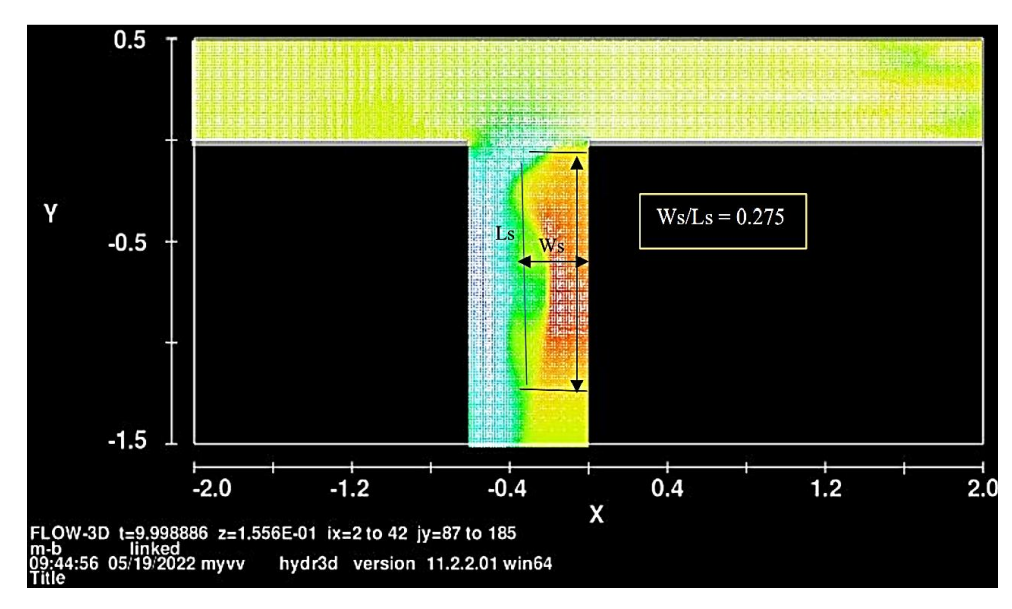


Figure 3: Shape Index at Qr=0.15, Fu= 0.3, Vu/Vc=0.45, $\theta = 90^{\circ}$, vu/B=0.31

In a figure 4, the angle that gives the highest values of the shape index (Ws\Ls) (the result of dividing the width (Ws) of separation zone by its length (Ls)) is the angle of 90, and the lowest values of the shape index were obtained at the angle of 60 and with a high discharge ratio (0.95) and the other angles, their shape index values range between these two angles.

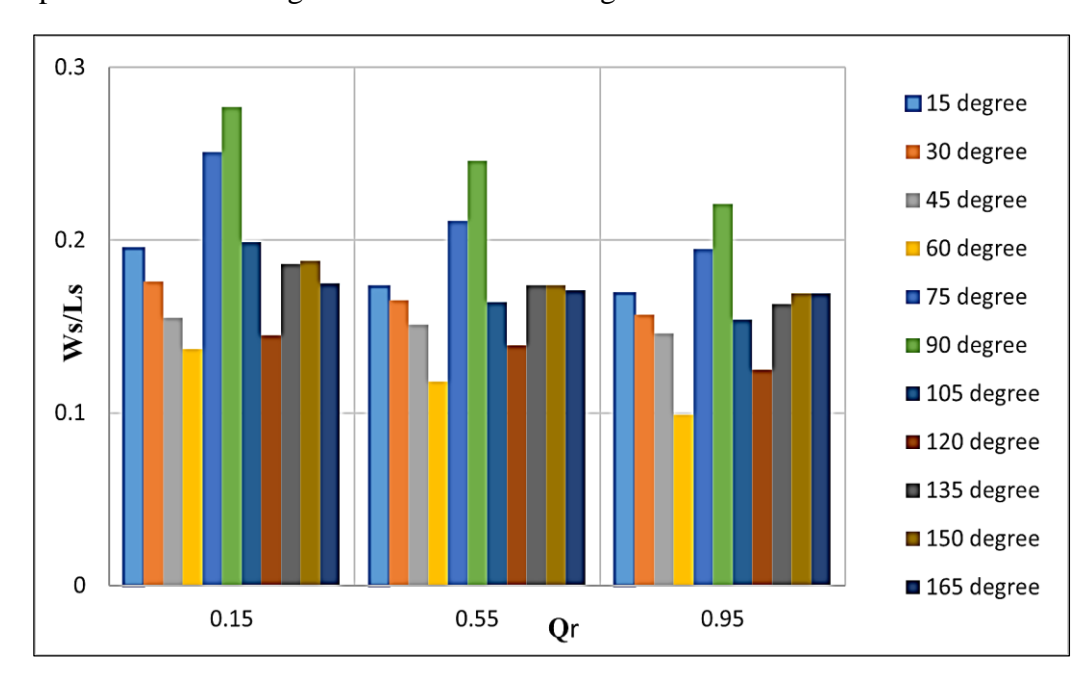


Figure 4: Influence of Discharge ratio on shape index at different angles.

3.2 Influence of Flow Intensity (Vu/Vc)

Velocity is a parameter that has a direct impact on the dimensions of the shape index. Where three values of the intensity of the flow (0.45, 0.85, and 1.2) were used to find out the effect of velocity

figures 5,6, and 7.

on separation zone, it was found through the results that increasing the flow intensity leads to an increase in the dimensions of the separation area, and an angle of 30 was chosen to illustrate this effect as in the

ISSN: 2709-6718

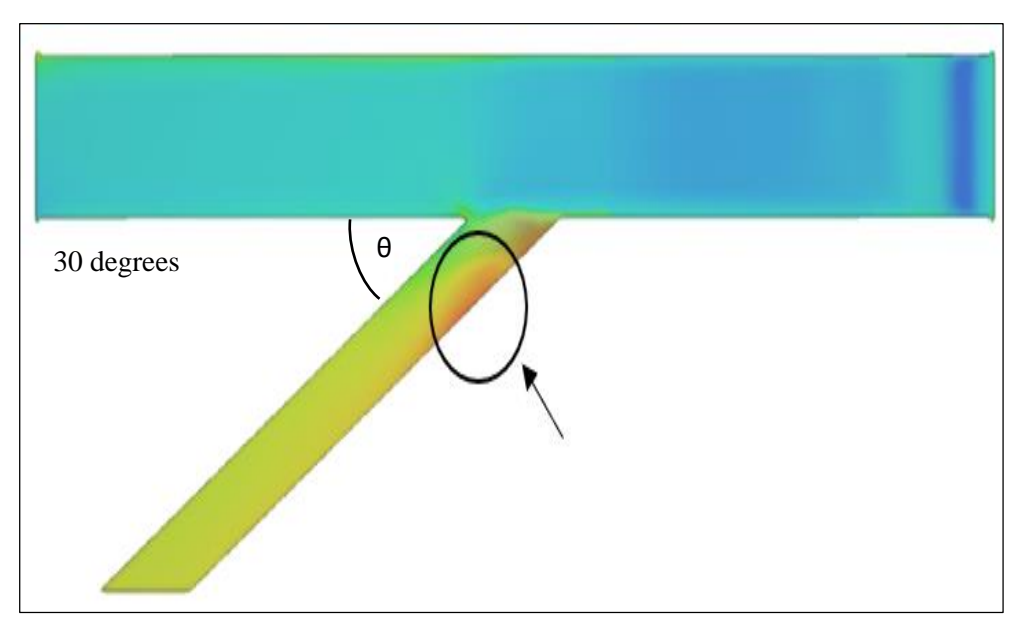


Figure 5: shape index at Vu/Vc=0.45, Fu=0.3, $\theta=75$ degree, Qr=0.95.

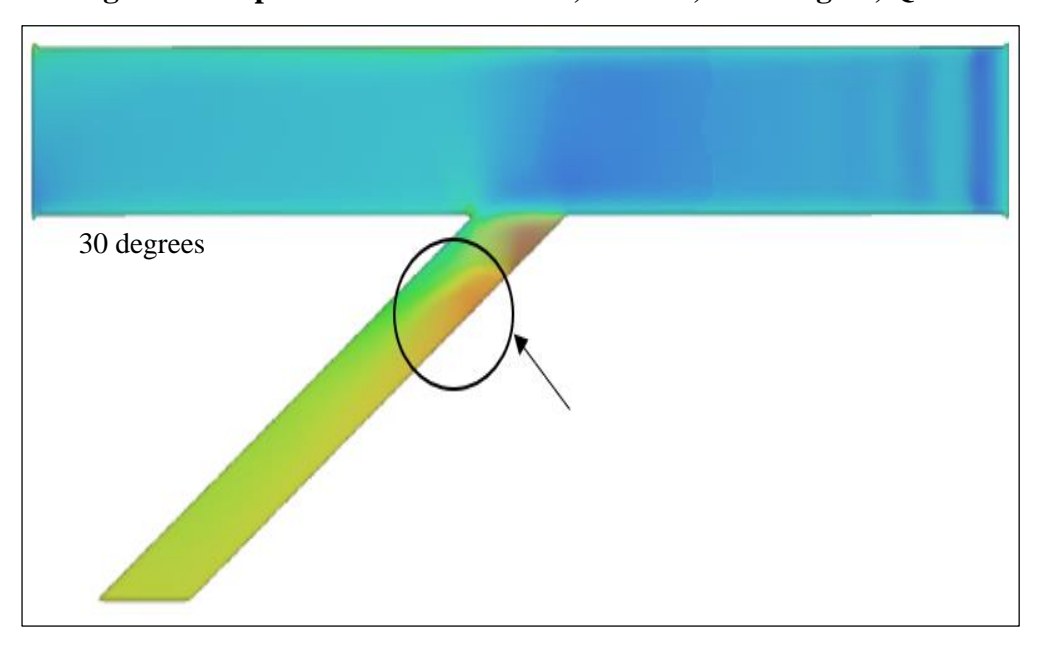


Figure 6: shape index at Vu/Vc=0.86, Fu=0.85, $\theta=75$ degree, Qr=0.95

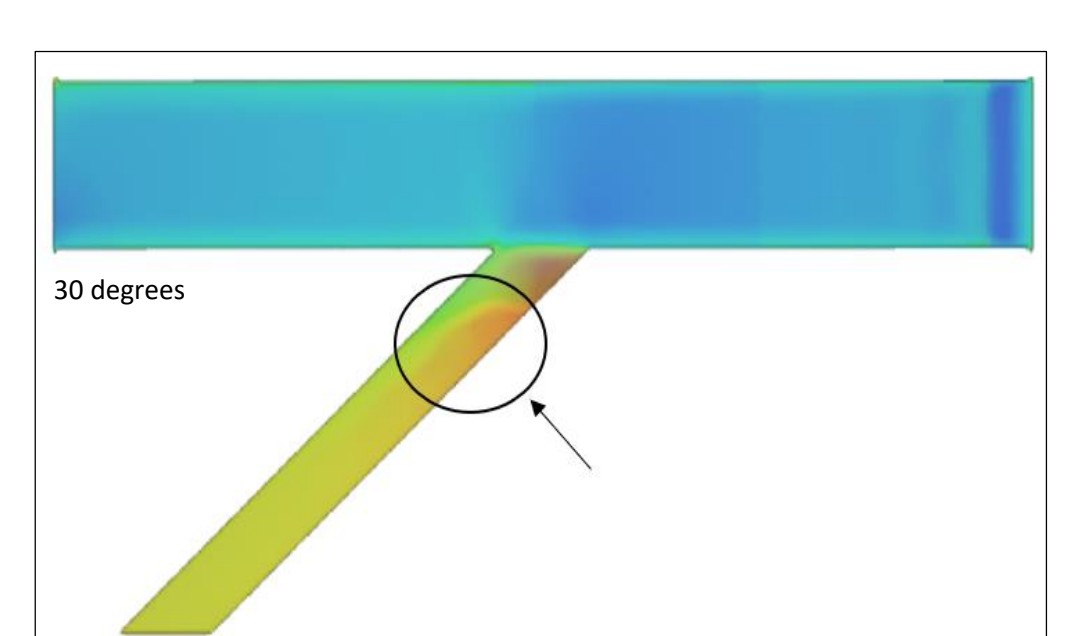


Figure 7: shape index at Vu/Vc=1.2, Fu=1.5, $\theta=75$ degree, Qr=0.95

The effects of flow velocity on the separation process at various angles and discharge ratios are depicted in figure 8. These figures clearly show that for each given branching angle, the size of the separation region grew in proportion to the rise in upstream velocity of the main channel. In addition, the velocity had a less effect on the angle of 60 compared to the other angles, with the largest dimensions of the separation region occurring at the angle of 90 for all discharge ratios.

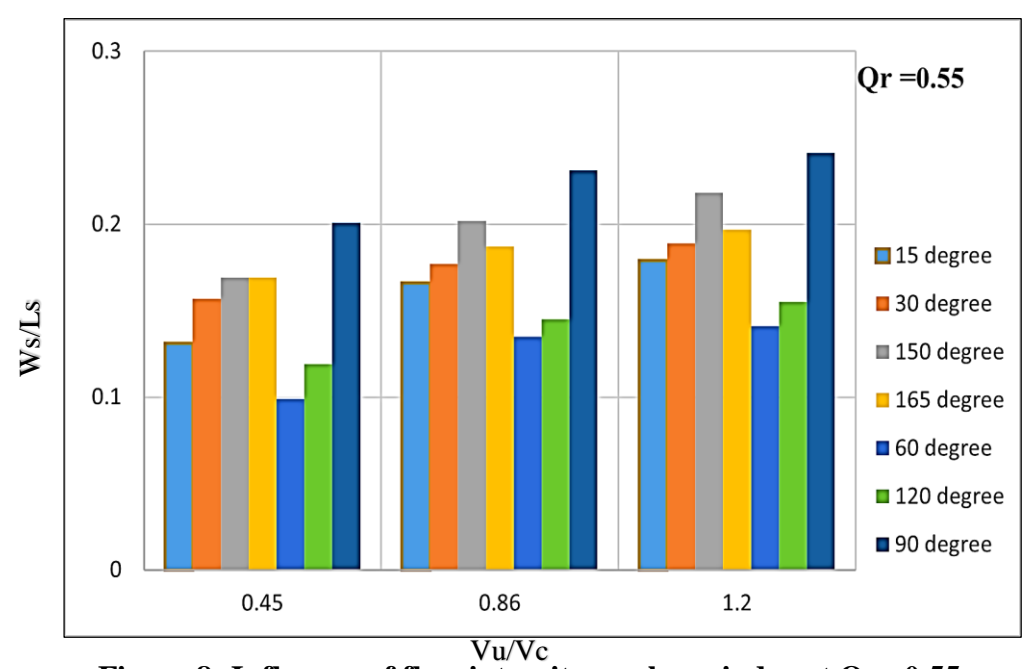


Figure 8: Influence of flow intensity on shape index at Qr = 0.55.

3.3 Influence of Upstream Froude Number (Fu)

Three Froud numbers (0.3, 0.85, and 1.5) were used, with the third value giving supercritical flow, because most academics interested in studying branching flow researched subcritical flow. Many runs are carried out with varying discharge ratios and for all branching angles to examine the impact of upstream Froude number. Figures 9,10, and 11 illustrating the impact of the Froude number on the shape index at a 45-degree angle are shown below.

ISSN: 2709-6718

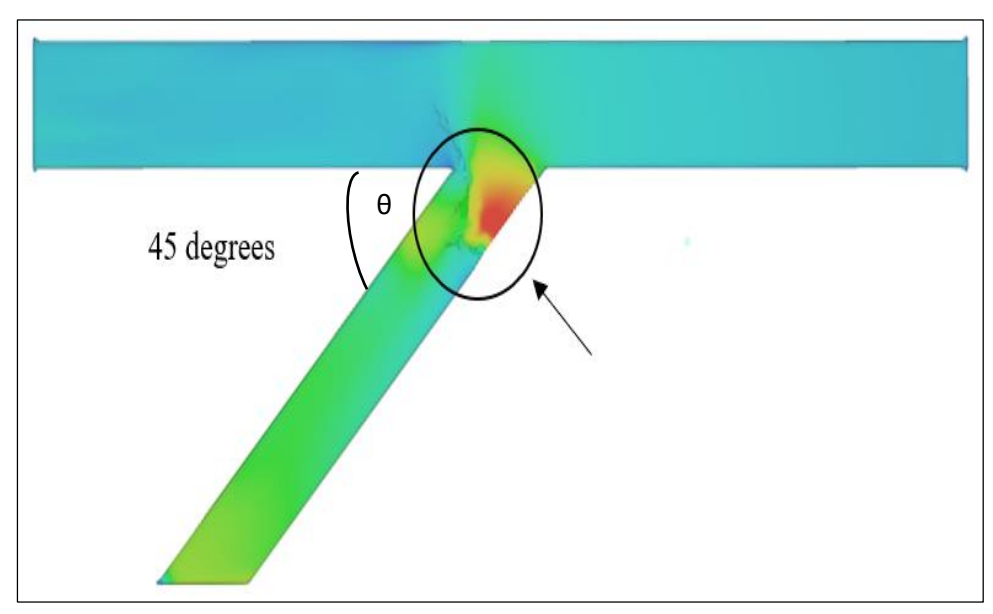


Figure 9: influence of upstream Froude number at discharge ratio =0.15, Fu=0.3, Vu/Vc =0.45

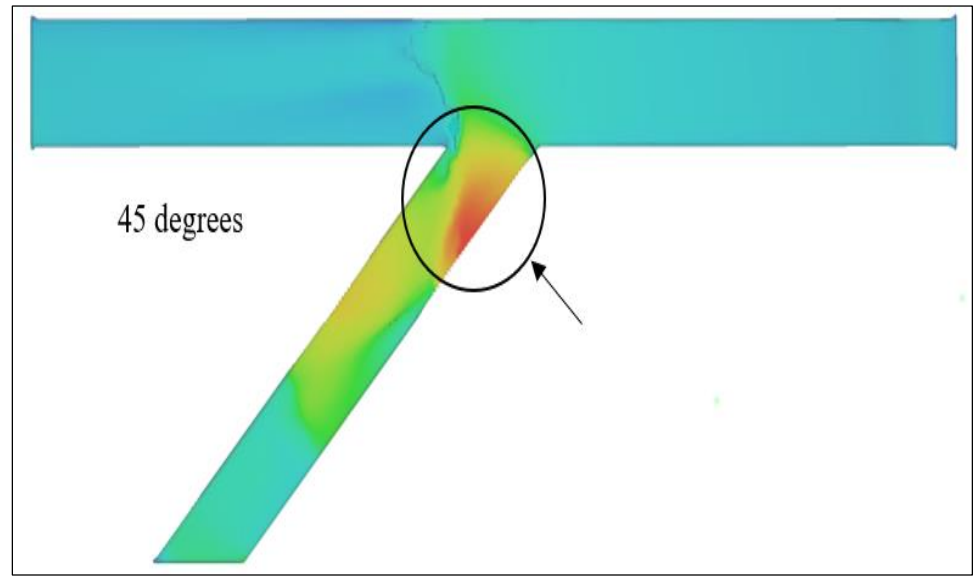


Figure 10: influence of upstream Froude number at discharge ratio =0.15, Fu=0.85, Vu/Vc =0.86

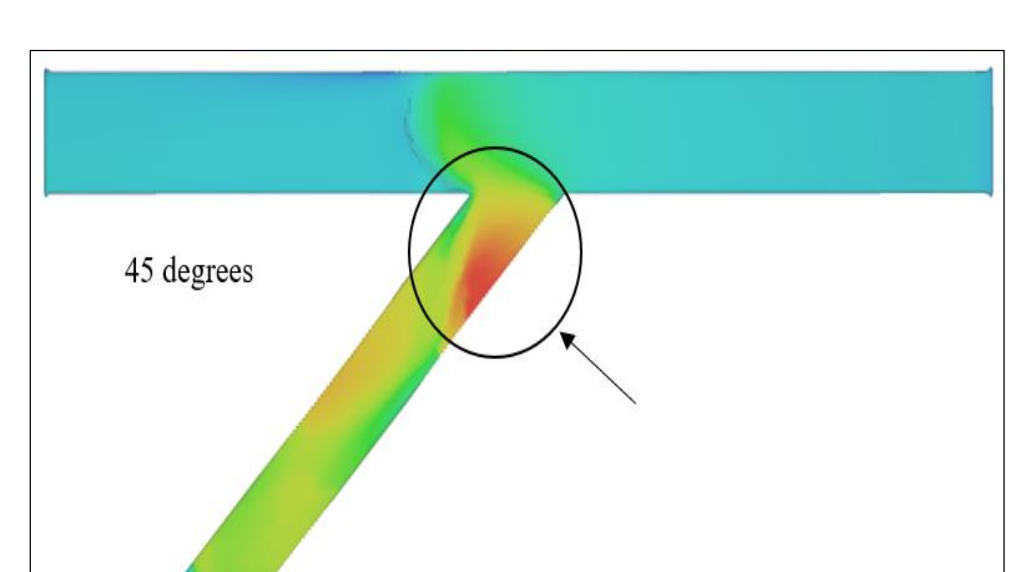


Figure 11: influence of upstream Froude number at discharge ratio =0.15, Fu=1.5, Vu/Vc =1.2 3.4 Influence of Depth Ratio (yu/B)

It has been found that the separation region develops larger in both directions as the depth of flow decreases, indicating an inverse relationship between the shape index and the depth of flow. The figures 12 and 13 exhibit the connection between the dimensions of the separation region and flow depth for various angles and discharge ratios, where three values of depth ratios (0.31, 0.16, 0.08) were utilized to show the effect of depth on separation zone. Where findings were consistent with prior attempts; where angle 60 gave the best outcomes.

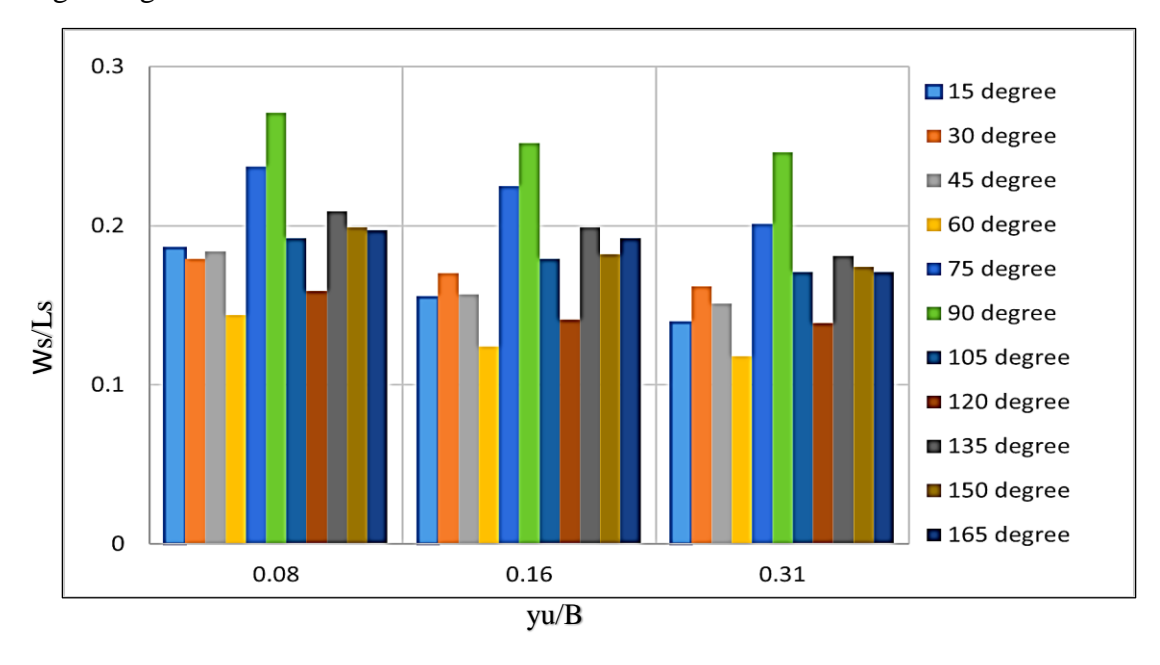


Figure 12: influence of flow depth at discharge ratio =0.55

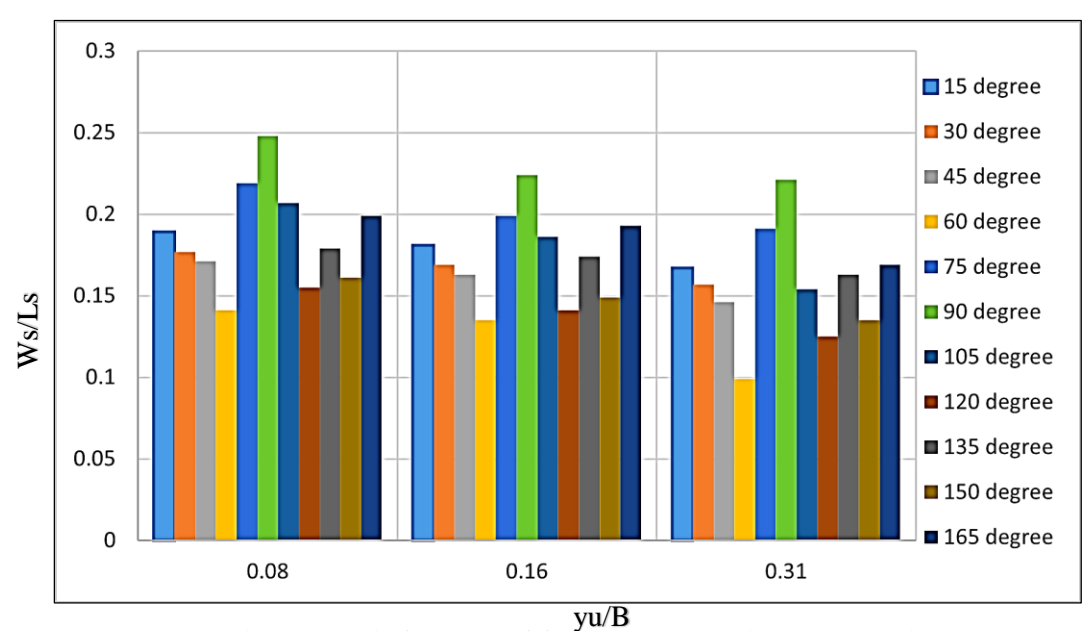


Figure 13: influence of flow depth at discharge ratio =0.95

Since the area of separation grows with decreasing water depth, Figure (12) displays bigger values for the shape index than Figure (13), which displays a larger discharge ratio. However, by employing a high discharge ratio, smaller regions can be obtained.

3.5 Influence of Branching Angle (θ)

The branching angle is the strongest parameter and thus the most influential shape index, and as such, it has a substantial effect on the size of the separation region. Small angles are preferred for better results and to prevent sediment accumulation at the entry of the branch channel, which is one of the most common challenges faced by engineers. Avoid using the angles of 15 and 30 degree when possible, since they are too steep to allow the entry of sufficient quantities of water to the branch channel and so result in overly wide separation regions. This research led to the conclusion that, for branch channel angles less than 90 degrees, the separation zone is formed downstream from the upstream, and for angles larger than 90 degrees, the separation region is upstream from the upstream. Moreover, as seen in the figures 14, 15, 16, 17, 18, and 19 the area of separation is minimized for angles below 90 degrees, while it is maximized for angles over 90 degrees, but remains smaller than the area that would be provided by an angle of 90 degrees.

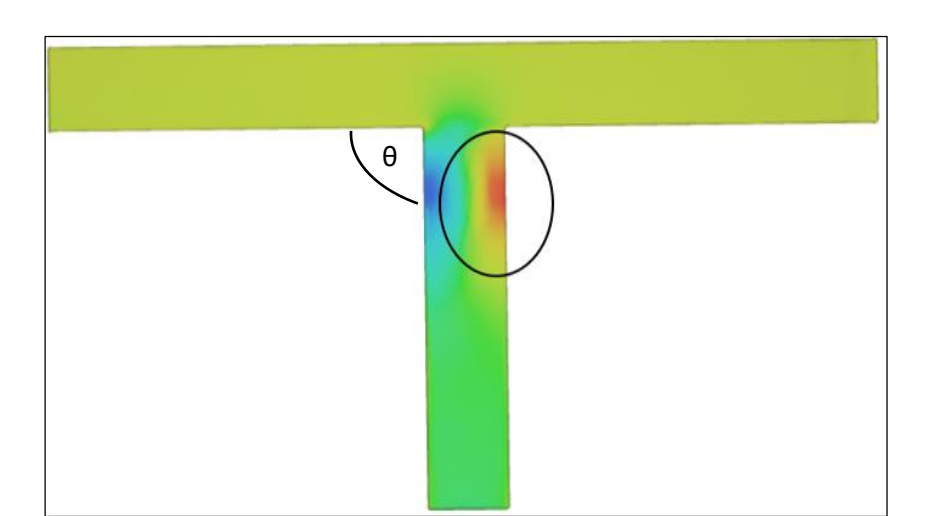


Figure 14: Separation zone size at 90 degrees

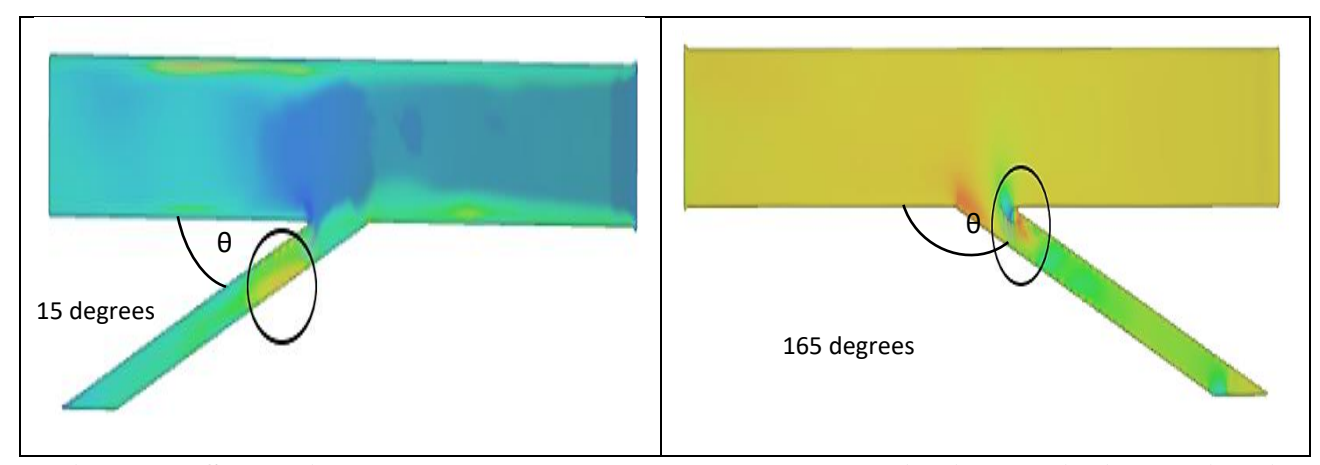


Figure 15: Separation zone at 15 degrees and the angle 165 which is opposite in the direction

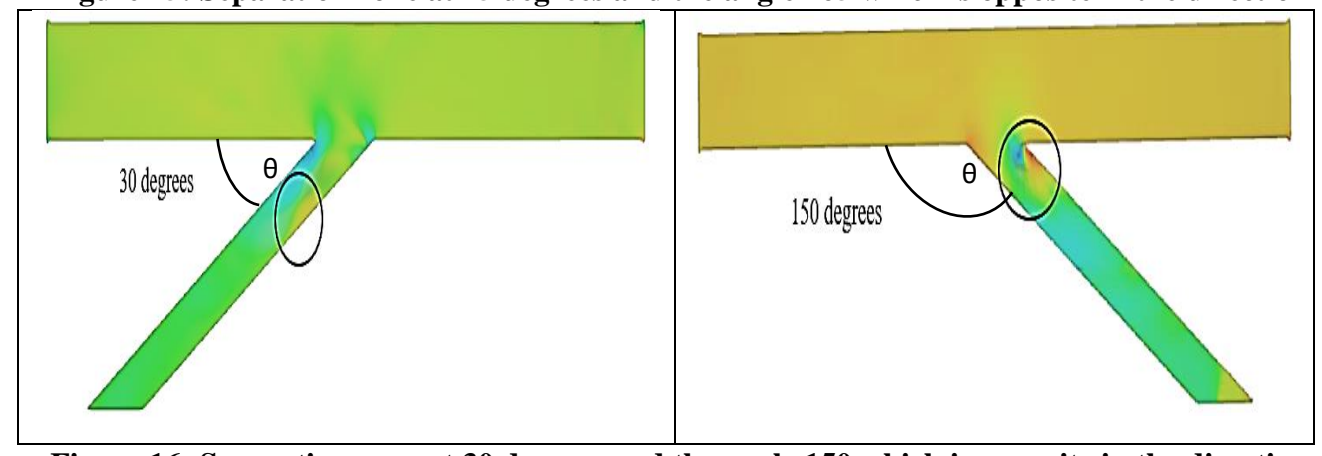


Figure 16: Separation zone at 30 degrees and the angle 150 which is opposite in the direction

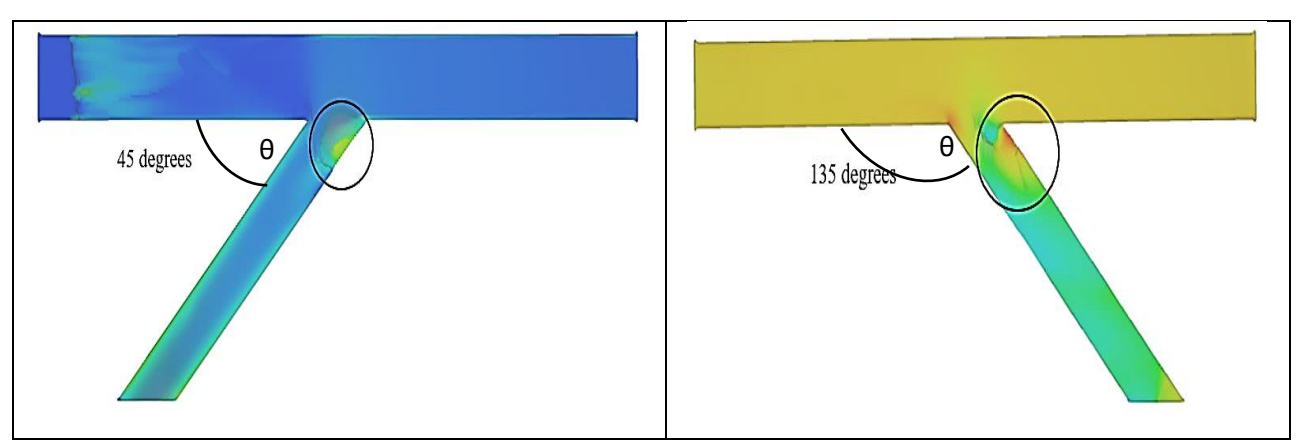


Figure 17: Separation zone at 45 degrees and the angle 135 which is opposite in the direction

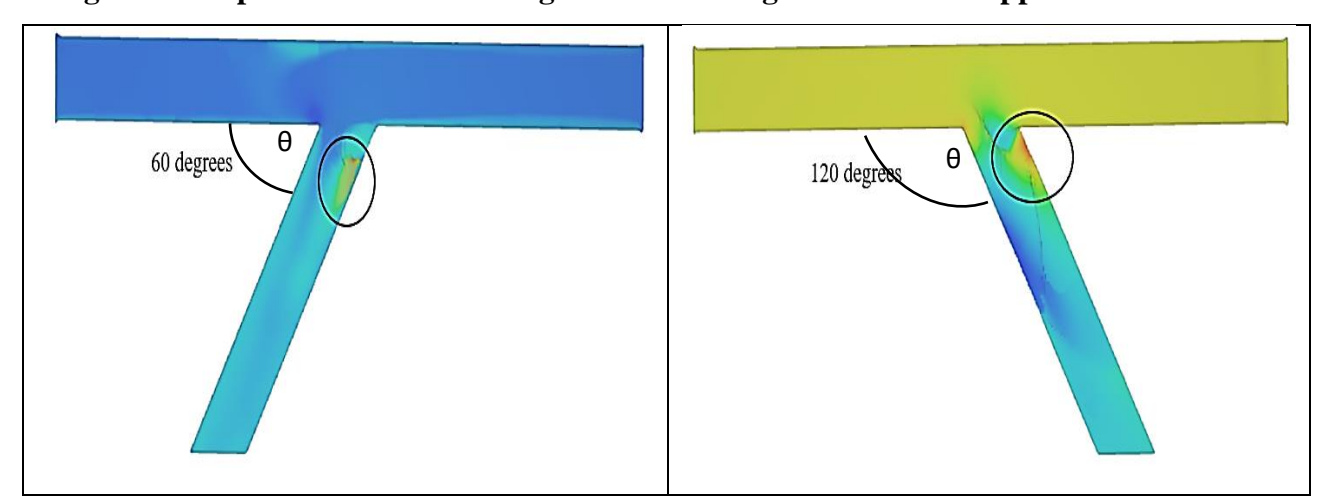


Figure 18: Separation zone at 60 degrees and the angle 120 which is opposite in the direction

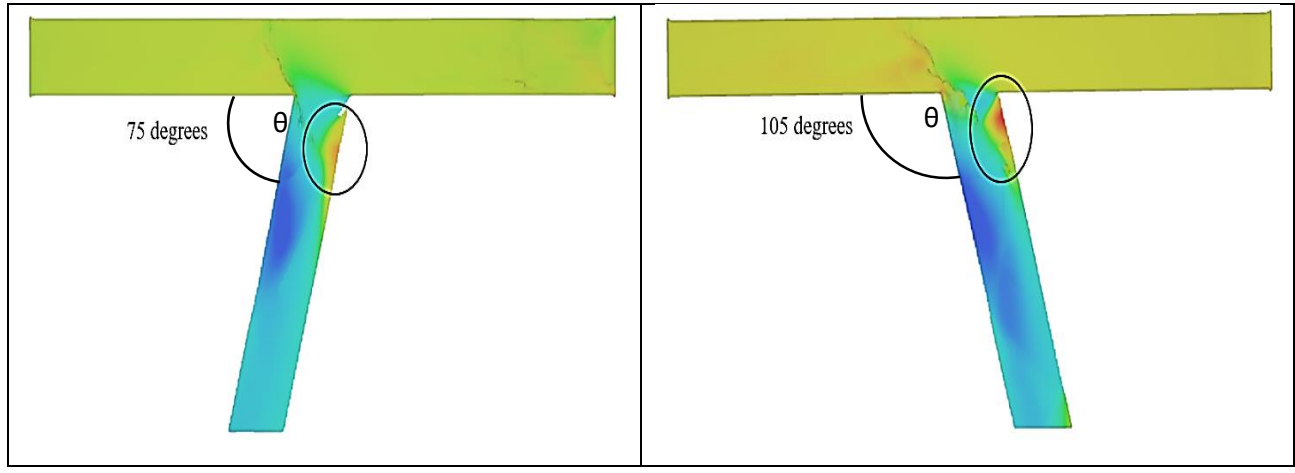


Figure 19: Separation zone at 75 degrees and the angle 105 which is opposite in the direction

Using the outputs of Flow 3D simulations, the impact of the branching angle was illustrated in the preceding graphics (14, 15, 16, 17, 18, and 19). Following are some figures that graphically depict the relationship between the branching angle and the separation zone for a variety of discharge ratios and flow intensities.

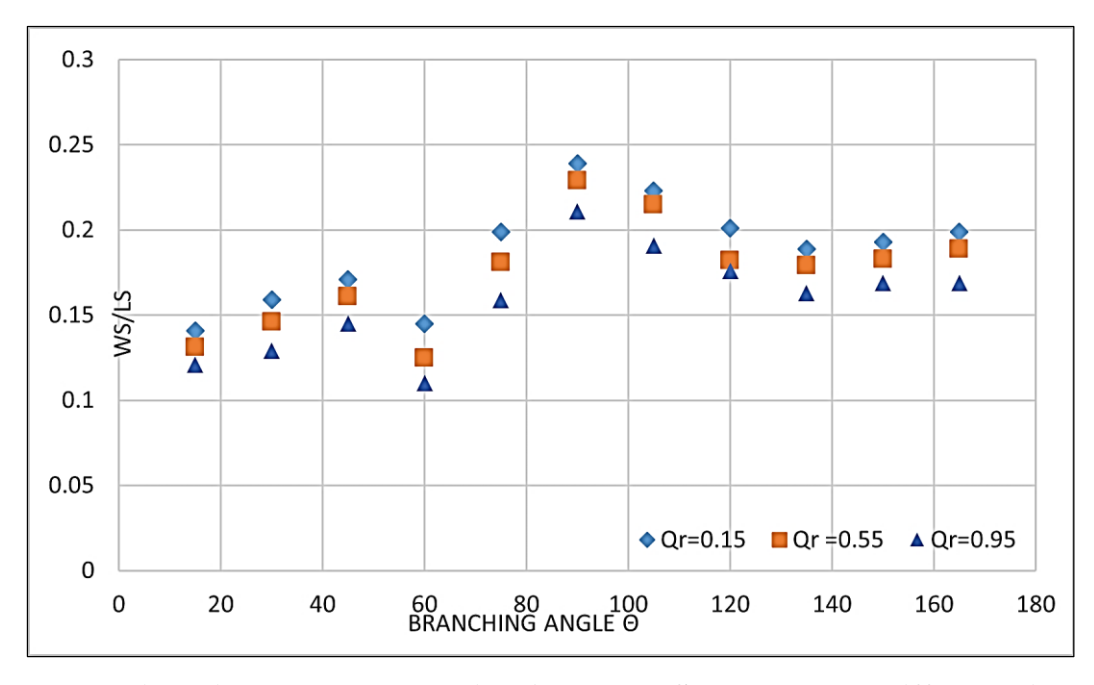


Figure 20: Relationship Between Branching Angle and Shape Index at different discharge ratios.

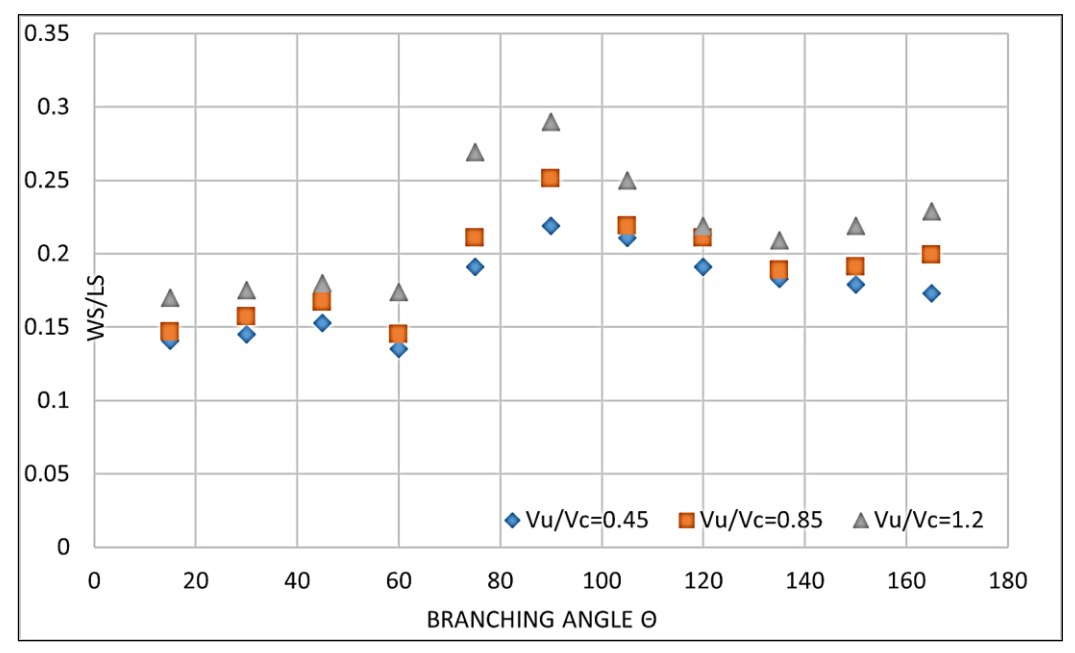


Figure 21: Relationship Between Branching Angle and Shape Index at different flow intensities.

It can be seen from the figures 20 and 21 that the optimum angle is 60 degrees because it gives smallest value of shape index.

4. Genetic Algorithm Theory (GEP Technique)

GEP is an emerging technique that builds on genetic programming by employing progressive artificial intelligence (AI). By supplying genomes in the form of linear, fixed-length chromosomes, GEP

combines the benefits of GP and GA in a model of phenotypes known as expression trees (ETs), which are similar to the trees used in GP analysis but have varied forms and sizes of branching structures [12]. In order to prepare such arithmetic functions, the GEP technique requires a data set to be input into the model, which is the approach's primary purpose. In the current investigation, the GEP model utilized a symbolic regression on the vast majority of GA genotypes to determine its output. Each chromosome in a specific primary population is first created at random and then subjected to a fitness function test against a predetermined set of fitness requirements. A vital part of the selection process is played by chromosomes with higher fitness values since they are more probable to be passed on to the following generation. As described in greater detail by Ferreira, selected chromosomes can be altered through the introduction of a wide range of genetic operations, including inversion, mutation, transposition of gene, root insertion sequence transformation (RIS), insertion sequence transposition (IS), rearrangement of the gene, and single or double crossover/recombination [12].

Changing chromosomes by mutation is the most common genetic modification. Thereafter, it's done again and again until either a desirable outcome is reached or a predetermined number of generations have elapsed [13]. The steps taken to develop this numerical modelling are shown in figure. (22). Recently, GEP technique has been put to use in a variety of contexts, including sewage sediment transportation [14], sentence ordering syntax [15], rain runoff model [16], hydraulic data prediction [17], time series modeling [18], Combining picture compression and multi-objective miners for a strong classification system [19]. To facilitate in the creation of GEP models for estimating the dimensions of separation zone at intake entrance, the present research made use of the potent software package GeneXproTools 5.0. By means of symbolic regression, GEP furnishes an arithmetic formula of the model to address the issue (function finding). Narrator can then utilize the resulting function to search for a term that adequately exemplifies the reliance.

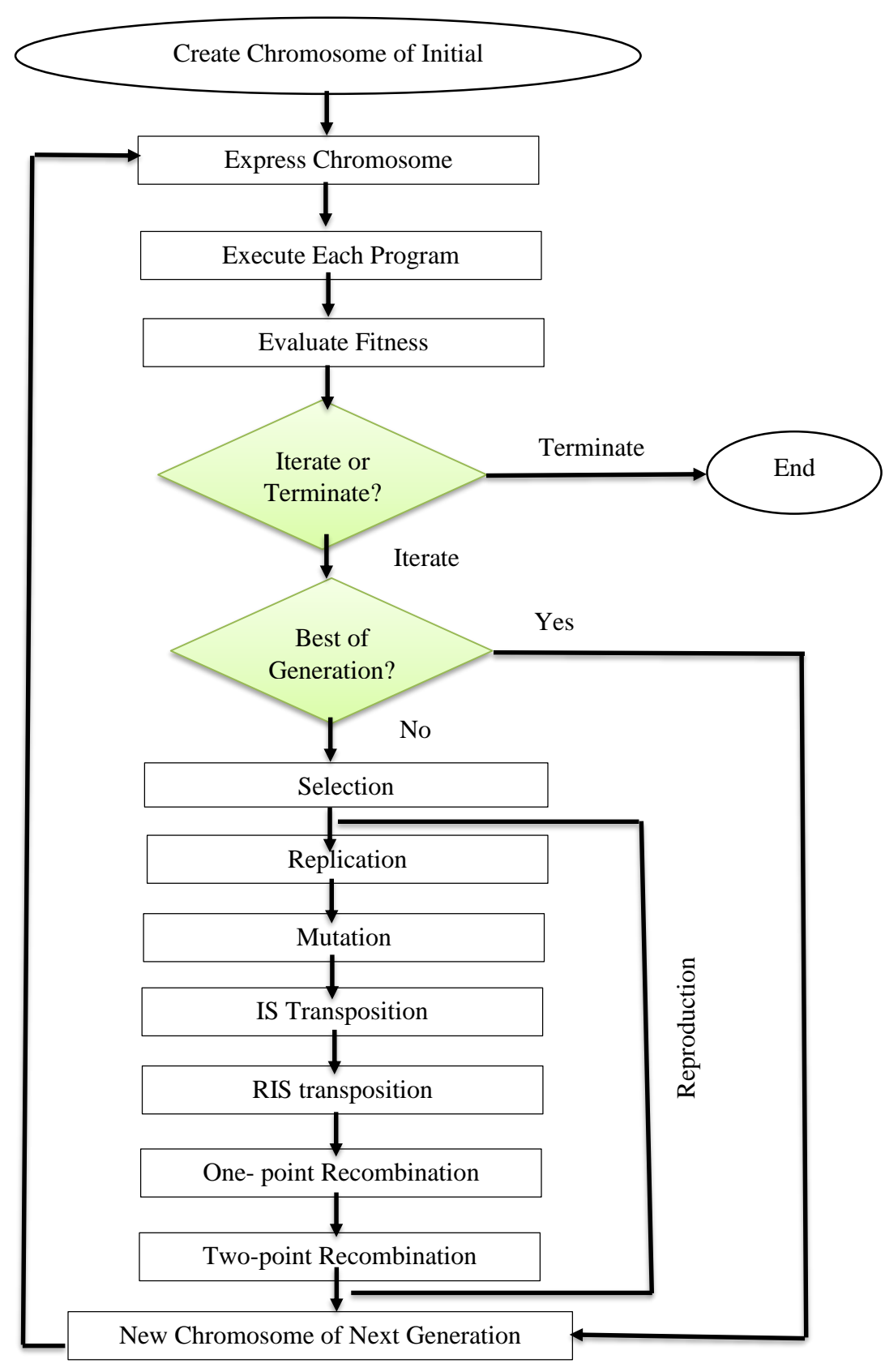


Figure 22: Flow diagram of Genetic Algorithm [14]

5. Models of Intake

5.1 GEP Model

Fifteen hundred datasets (Obtained from Flow-3d Software) were gathered and numerically simulated with flow-3d to create the GEP model for predicting separation region dimensions. After collecting the necessary information represented by a dependent variable (Ws/Ls) and independent variables (Vu/Vc, Fu, Qr, yu/B, θ), the GEP was used to create the Ws/Ls model. The GEP randomized the data into training data (80%) and validation/testing data (20%) sets. The training data was then used to train the GEP model. Six stages were taken to define GEP parameters and processes in order to generate the statistical model needed to anticipate shape index. The first thing that had to be done was to fix a sample population. In this phase, any population size is acceptable; however, research by Ferreira [12] suggests that populations of 30 to 100 produce the best outcomes. Multiple iterations were performed to determine the optimal number, and 45 chromosomes was chosen for the study population since it yielded the most accurate findings. The root-mean-square error (RMSE) was then used to evaluate the fitness function of each chromosome. Step three involved categorizing each gene on the chromosome into functional and terminal subsets. The final solution relied on a terminal set T = (Fu, Vu/Vc, Qr, yu/B, X), where X represented the random numerical constant (RNC), and a function set $F = (\sin, +, -, *, /)$ for the arithmetic and some mathematical operations. The fourth procedure dealt with the chromosome structure based on the chosen head length and genes number; according to Ferreira, increasing the gene number in a chromosome from 1 to 3 aids in increasing its success rate [12]. Finally, five different freeform float types (Dc) were used to represent the random numerical constants in the range (-10 to 10). Due to the fact that there are three genes per chromosome, the final equation of these sub-ETs was connected by addition (+). This study made use of a wide variety of genetic techniques, including transposition (transposition of gene, IS, and RIS), mutation (recombination rate of gene, one point and two-points recombination rate), and inversion rate. Table (2) contain the genetic operations of the model.

ISSN: 2709-6718

Table 2: Genetic Operations of the Model

Parameter	Value
Population size	45
Terminal set	+, -, *, /, sin
Function set	Fu, Vu/Vc, yu/B, Qr, θ, X
Random numerical constant (RNC)	5
Type of RNC	Floating point
RNC range	[-10, 10]

Head length	8
Number of genes	3
Function of linking	Addition
Function of fitness	RMSE
Mutation rate	0.033
Inversion rate	0.11
IS transposition rate	0.11
RIS transposition rate	0.11
Gene transposition rate	0.11
One-point recombination rate	0.11
Two-point recombination rate	0.33
Gene recombination rate	0.33
Dc-specific mutation rate	0.033
Dc-specific inversion rate	0.11
Dc-specific IS transposition rate	0.11
Random constant mutation rate	0.01

GeneXproTools 5.0 was used to run simulations of the model for more than 55,000 generations once all genetic parameters had been determined. The expression tree (ET) representation of the resulting shape index (Ws/Ls) equation can be seen in figure (23), while the corresponding equation is provided in Eq (3).

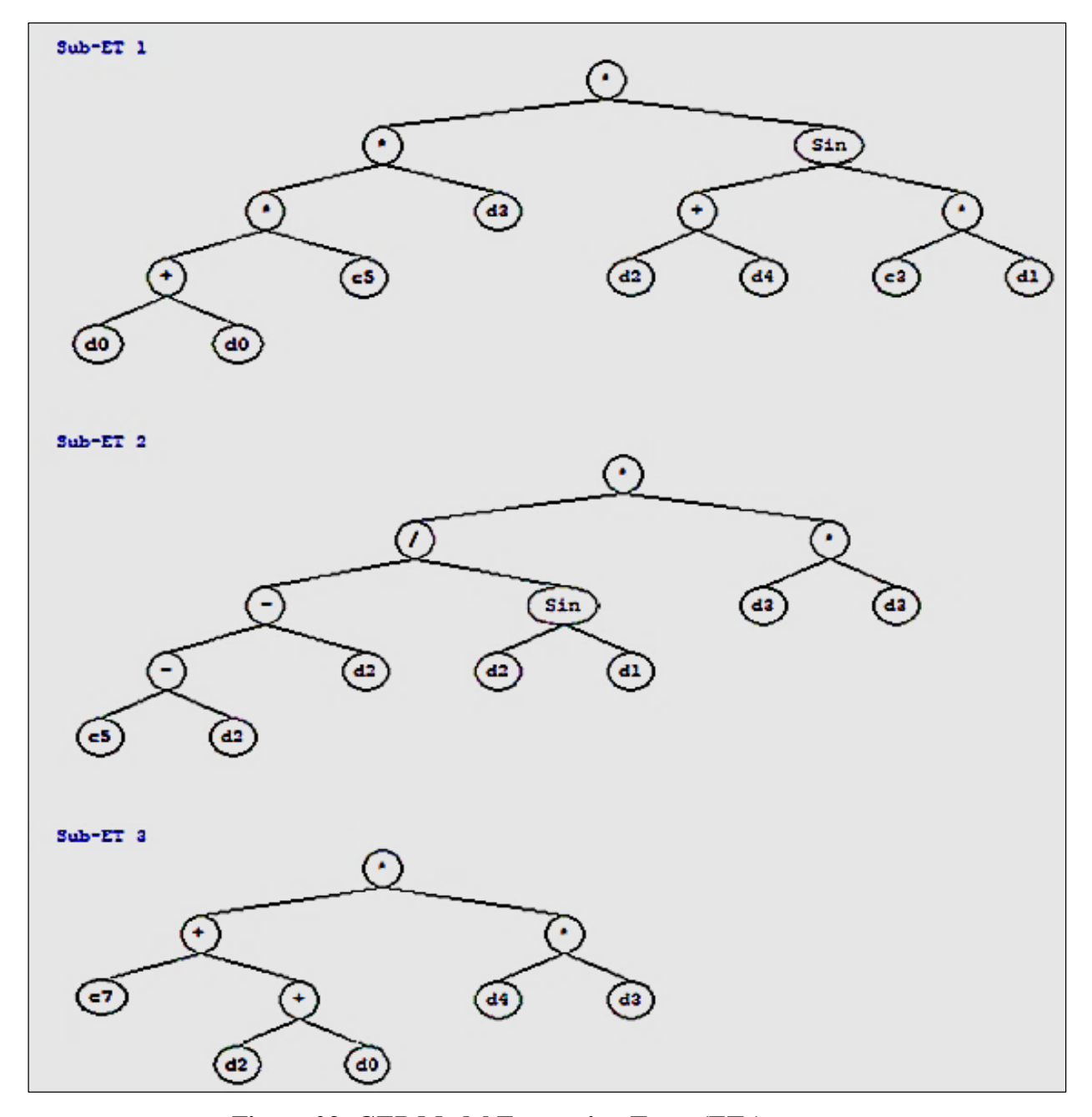


Figure 23: GEP Model Expression Trees (ETs)

$$\frac{Ws}{Ls} = \left[2d_0 * c_5 * d_3\right] * \left[d_2 + d_4\right] sin(c_3 * d_1) + \left[\frac{c_5 - 2d_2}{d_2 sind_1}\right] * d_3^2 + \left[c_7 + d_2 + d_0\right] * d_4
* d_3$$
(3)

The following table contain the parameters which used in eq. (3)

Table 3: Definition of ET Parameters

Parameters	Definition
1	0.
d_{o}	Qr
d_1	θ
d_2	Yu/B
\mathbf{d}_3	Fu
d ₄	Vu/Vc
C ₃	1.01
C ₅	0.7
C ₇	0.12

5.2 Predicting Model of NLR

The necessary data that which used in non-linear regression (NLR) model were split in a technique similar to the dividing of the data of the generalized estimating equations (GEP) model (training and testing data sets). Firstly, a linear model was tried out as part of this forecasting structure; however, its low R^2 value of 0.64 indicates that it is not a reliable predictor. Moreover, it was discovered that nonlinear models were the only ones capable of making accurate predictions. Thus, the connection between the shape index (Ws/Ls) and the other free parameters is seen in Equation (4) with R^2 of 0.833.

$$\frac{Ws}{Ls} = 0.301 + 0.15 * Qr + 0.213 * \frac{V_u}{V_c} + 0.156 \frac{y_u}{B} + 0.08 sin\theta - 0.025 * F_u^2 - 0.018 * Q_r^2$$

$$+0.17\frac{V_{u}}{V_{c}}*sin\theta \tag{4}$$

6. Discussion of the Results

The main goal of this study is to find the optimum intake angle and compare the accuracy of predictions made by the GEP model and those made by the NLR model. The optimal angle, according

to the simulation results, is 60 degrees, which yields the lowest value of the shape index at all cases. Data from Flow-3D numerical simulation software was utilized to collect a total of 150 cases, from which a new formula of shape index based on GEP and NLR models was derived. Scatterplots in Figures (24,25) depict the projected shape index versus measured shape index, which was obtained using both the GEP and NLR models for the training and testing data sets. The objective of employing dissipatedly plots was to analyze the level of correspondence between the measured and the predicted values some more intuitionally. Three statistical measures (R², MAE, and RMSE) were also calculated for each model, as illustrated Table 4. Table (4) displays statistical findings that imply GEP outperforms NLR by determining which equation provides the minimum errors in prediction. GEP model results in greater value of R², and lower value of RMSE and MAE and less dispersion around the acceptance line than the model of NLR. Eq. (3) represents a straightforward experimental representation of the shape index model, which is made possible by the GEP model's special characteristics. Although NLR's model performed less well than GEP's, it was still satisfactory. This condensed and clear mathematical formulation is thus GEP's main contribution, and it will likely be valuable for future designers.

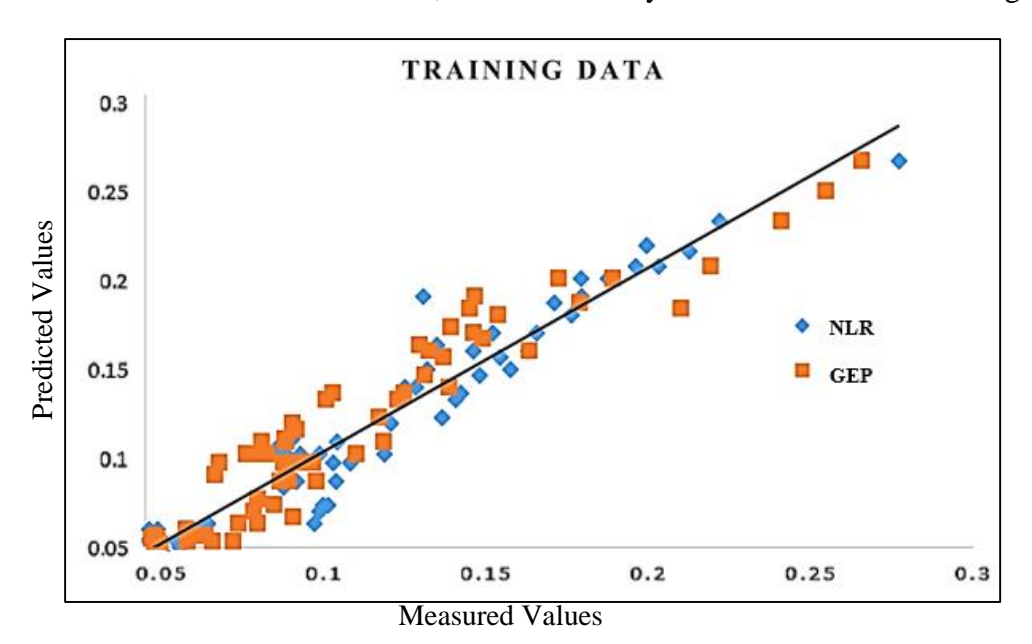


Figure 24: Comparative of GEP and NLR for Training Group (Shape index Data).

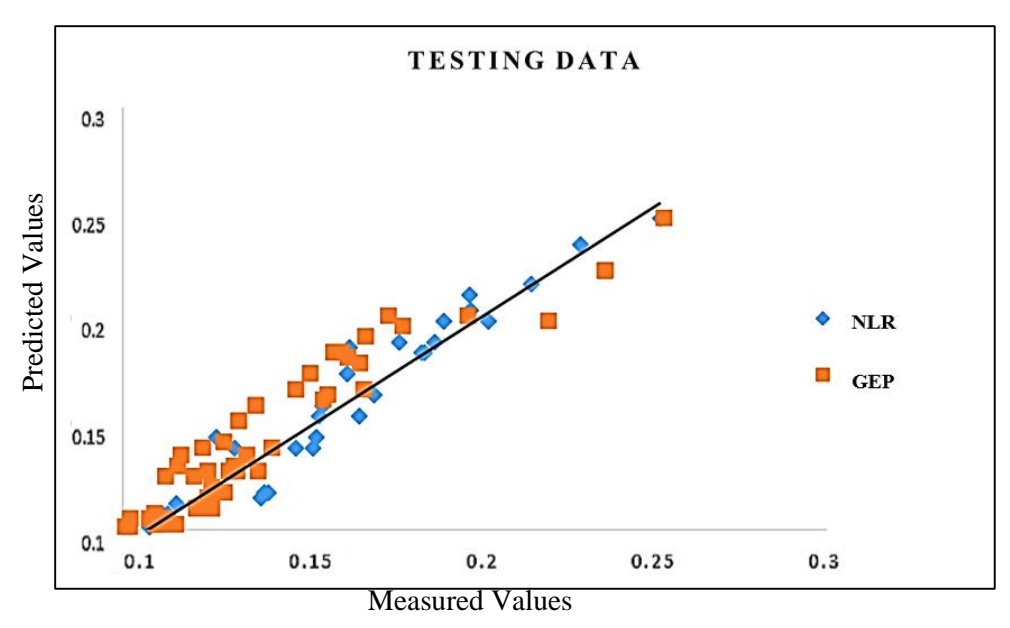


Figure 25: Comparative of GEP and NLR for Testing Group (Shape Index Data).

Testing Model **Training Type** Group Group R^2 R^2 **RMSE MAE RMSE MAE NLR** 0.145 0.119 0.852 0.151 0.122 0.833 **GEP** 0.105 0.087 0.907 0.109 0.092 0.903

Table 4: Results of statistic for both models of NRL and GEP.

7. Conclusion

An essential necessity properly estimates the size of separation none to prevent the intake entry from becoming clogged with deposited sediments, but the separation process that occurs at intakes represents a complicated flow structure that can be problematic to evaluate. The angles of water intake were varied from 15 to 165 degree. Lastly, it was found that the optimum angle for installation a channel intake is 60°. Furthermore, the performance of GEP and NLR was compared using mathematical models generated from numerical simulations and the resulting 150 data sets. According to Table 4, the results revealed that the shape index formula produced from the model of Gene expression programing performed better than that derived using the traditional nonlinear regression model. The GEP reduced the RMSE (0.109) and the MAE (0.092) and increased the R² value (0.903). Moreover, the GEP model was distinguished by a simple, compact equation that could be readily implemented by engineers. The GEP approach is superior to the NLR model because of this characteristic. Because of this, the GEP model is a useful modeling tool for estimating the size of the separation zone, and also provides a

straightforward empirical formula for the modeled response function. Consequently, designers can use Equation 3 which acquired from the GEP model, to determine the smallest possible separation zone at intakes under scenarios like those considered in this research. The parameters restrictions for Eq. (3) which involved Froude number (0.3 to 1.5), discharge ratio (0.15 to 0.95), flow intensity (0.45 to 1.2), water depth (0.08 to 0.31), and branching angle (15 to 165). Researchers are encouraged to expand on Eq. (3) by investigating the impact of varying ranges of channel width ratio, channel slope, and different channel bed level on the separation process.

ISSN: 2709-6718

References

- [1] A. Keshavarzi and L. Habibi, "Optimizing water intake angle by flow separation analysis," *Irrigation and Drainage: The journal of the International Commission on Irrigation and Drainage,* vol. 54, no. 5, pp. 543-552, 2005, doi: https://doi.org/10.1002/ird.207.
- [2] W. H. Al-Mussawi, "Numerical analysis of velocity profile and separation zone in open channel junctions," *Al-Qadisiyah Journal for Engineering Sciences*, vol. 2, no. 2, pp. 262-274, 2009.
- [3] M. Heydari and S. Shabanlou, "The effects of flow division angle in rectangular channel branches," *Water and Soil Science*, vol. 30, no. 1, pp. 193-204, 2020, doi: https://dor.isc.ac/dor/20.1001.1.20085133.1399.30.1.15.1.
- [4] FLOW-3Dmanual, "FLOW-3D user manual," N. Flow Science Santa Fe, Ed., ed, 2017.
- [5] M. Muzzammil, J. Alama, and M. Danish, "Scour prediction at bridge piers in cohesive bed using gene expression programming," *Aquatic Procedia*, vol. 4, pp. 789-796, 2015, doi: https://doi.org/10.1016/j.aqpro.2015.02.098.
- [6] M. Najafzadeh and G.-A. Barani, "Comparison of group method of data handling based genetic programming and back propagation systems to predict scour depth around bridge piers," *Scientia Iranica*, vol. 18, no. 6, pp. 1207-1213, 2011, doi: https://doi.org/10.1016/j.scient.2011.11.017.
- [7] H. M. Azamathulla, A. A. Ghani, N. A. Zakaria, and A. Guven, "Genetic programming to predict bridge pier scour," *Journal of Hydraulic Engineering*, vol. 136, no. 3, p. 165, 2010, doi: https://doi.org/10.1061/(ASCE)HY.1943-7900.0000133.
- [8] M. Najafzadeh and H. M. Azamathulla, "Neuro-fuzzy GMDH to predict the scour pile groups due to waves," *Journal of Computing in Civil Engineering*, vol. 29, no. 5, p. 04014068, 2015, doi: https://doi.org/10.1061/(ASCE)CP.1943-5487.0000376.
- [9] M. Khan, H. M. Azamathulla, and M. Tufail, "Gene-expression programming to predict pier scour depth using laboratory data," *Journal of Hydroinformatics*, vol. 14, no. 3, pp. 628-645, 2012, doi: https://doi.org/10.2166/hydro.2011.008.
- [10] Y. A. M. Moussa, "Modeling of local scour depth downstream hydraulic structures in trapezoidal channel using GEP and ANNs," *Ain Shams Engineering Journal*, vol. 4, no. 4, pp. 717-722, 2013, doi: https://doi.org/10.1016/j.asej.2013.04.005.
- [11] A. Ramamurthy, J. Qu, and D. Vo, "Numerical and experimental study of dividing open-channel flows," *Journal of Hydraulic Engineering*, vol. 133, no. 10, pp. 1135-1144, 2007, doi: https://doi.org/10.1061/(ASCE)0733-9429(2007)133:10(1135).
- [12] C. Ferreira, *Gene expression programming: mathematical modeling by an artificial intelligence*. Springer, 2006.
- [13] C. Ferreira, "Gene expression programming: a new adaptive algorithm for solving problems," *arXiv* preprint cs/0102027, 2001, doi: https://doi.org/10.48550/arXiv.cs/0102027.

- [14] A. Ab. Ghani and H. Md. Azamathulla, "Gene-expression programming for sediment transport in sewer pipe systems," *Journal of pipeline systems engineering and practice,* vol. 2, no. 3, pp. 102-106, 2011, doi: https://doi.org/10.1061/(ASCE)PS.1949-1204.0000076.
- [15] Z. Xie, X. Li, B. Di Eugenio, W. Xiao, T. M. Tirpak, and P. C. Nelson, "Using gene expression programming to construct sentence ranking functions for text summarization," in *COLING 2004: Proceedings of the 20th International Conference on Computational Linguistics*, 2004, pp. 1381-1384.
- [16] A. Fernando, A. Shamseldin, and R. Abrahart, "Using gene expression programming to develop a combined runoff estimate model from conventional rainfall-runoff model outputs," in *Proc., 18th World IMACS Congress and MODSIM09 International Congress on Modelling and Simulation*, 2009, pp. 2377-2383, doi: http://mssanz.org.au/modsim09.
- [17] K. A. Eldrandaly and A.-A. Negm, "Performance Evaluation of Gene Expression Programming for Hydraulic Data Mining," *Int. Arab J. Inf. Technol.*, vol. 5, no. 2, pp. 126-131, 2008.
- [18] A. Bărbulescu and E. Băutu, "Time series modeling using an adaptive gene expression programming algorithm," *International journal of mathematical models and methods in applied sciences,* vol. 3, no. 2, pp. 85-93, 2009.
- [19] S. Dehuri and S.-B. Cho, "Multi-objective classification rule mining using gene expression programming," in *2008 Third International Conference on Convergence and Hybrid Information Technology*, 2008, vol. 2: IEEE, pp. 754-760, doi: https://doi.org/10.1109/ICCIT.2008.27.

التنبؤ بالزاوية المثلى للمأخذ عند تقاطع القناة المفتوحة باستخدام تقنية برمجة التعبير الجينى

ISSN: 2709-6718

الخلاصة: عادة ما تستخدم مداخل المياه لتحويل المياه من القناة الرئيسية أو النهر إلى القنوات الثانوية وأنظمة التوربينات. في الحالات التي يتم فيها فصل التدفق عند مدخل القناة الفرعية، يكون هيكل التدفق في هذه المنطقة أكثر تعقيدًا من الأجزاء الأخرى من الشبكة. في الغالب، يتم بناء المداخل بزوايا قائمة، مما يخلق منطقة فصل كبيرة عند مدخل القناة الفرعية ويقلل من تصريف التدفق. من أجل تقليل أبعاد منطقة الفصل، يجب وضع المدخل بأفضل زاوية ممكنة. أجريت دراسة عددية في قناة مستطيلة مع قناة جانبية تتفرع منها لتحديد زاوية السحب المثلى. تم تركيب أحد عشر مدخلًا على جانب واحد من القناة الرئيسية بزوايا متفاوتة 15 و 30 و 45 و 90 و 105 و 100 و 105 و 150 و 165 و 160 درجة للعثور على موضع السحب الأمثل. بالإضافة إلى ذلك، تم اقتراح طريقة فريدة لتقدير أبعاد منطقة الفصل باستخدام نهج نمذجة الحوسبة الدقيقة المتقدم والمسمى برمجة التعبير الجيني (GEP). وطبقا لنتائج هذه الدراسة، تم استخدام فريدة الرقمية لإجراء مقارنة بين نموذج GEP ونموذج الانحدار غير الخطي (NLR). تشير قيم RMS وRMSE وRMSE و MAE و 0.092 و MAE و 0.092 و MAE و 0.093 و المنافقة باستخدام برنامج GEP متفوقة على صيغة NLR (0.903 و 100 و 10